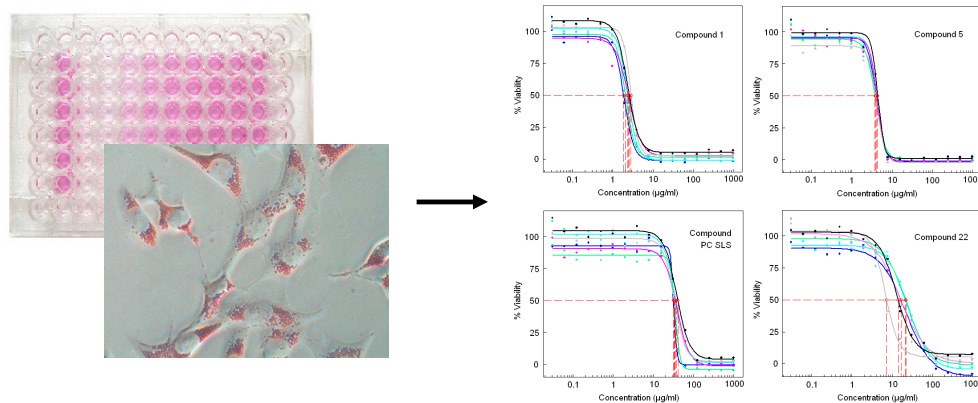JRC Scientific and Technical Reports

A biology-based dynamic approach for the modelling of toxicity in cell-based assays. Part I: Fate modelling

J. M. Zaldívar, M. Mennecozzi, R. Rodrigues and M. Bouhifd

JRC
EUROPEAN COMMISSION

Institute for Health
and Consumer Protection

The mission of the IHCP is to provide scientific support to the development and implementation of EU policies related to health and consumer protection.

The IHCP carries out research to improve the understanding of potential health risks posed by chemical, physical and biological agents from various sources to which consumers are exposed.

***Europe Direct is a service to help you find answers
to your questions about the European Union***

Freephone number (*):

00 800 6 7 8 9 10 11

(*) Certain mobile telephone operators do not allow access to 00 800 numbers or these calls may be billed.

A great deal of additional information on the European Union is available on the Internet.
It can be accessed through the Europa server http://europa.eu/

Printed in Italy

EXECUTIVE SUMMARY

There is a need to integrate existing *in vitro* dose-response data in a coherent framework for extending their domain of applicability as well as their extrapolation potential. This integration would contribute towards the reduction of animal use in toxicology by using *in vitro* data for quantitative risk assessment; moreover it would reduce costs and time especially when such approaches would be used for dealing with complex human health and ecotoxicological endpoints. In this work, based on HTS (High Throughput Screening) *in vitro* data, we have assessed the advantages that a dynamic biology-toxicant fate coupled model for *in vitro* cell-based assays could provide when assessing toxicity data, in particular, the possibility to obtain the dissolved (free) concentration which can help in raking the toxicity potency of a chemical and improve data reconciliation from several sources taking into account the inherent variability of cell-based assays. The results show that this approach may open a new way of analyzing this type of data sets and of extrapolating the values obtained to calculate *in vivo* human toxicology thresholds.

CONTENTS

1. INTRODUCTION

The hazard assessment of a chemical has traditionally relied on animal models, with protocols that have been standardized over the years (OECD, 1993), and in the application of assessment factors (AFs) to take into account uncertainties associated with the extrapolation of animal model results to humans. However, during the last years, integrated testing strategies (ITS) have gained a considerable interest in toxicology (Worth, 2004; Balls et al., 2006; van Leeuwen, et al., 2007) due principally to new *in vitro* and *in silico* technologies and methods, to new knowledge generated (web databases), to new insight on the mechanisms of toxic effects, e.g. toxicogenomics (Heijne et al., 2005), systems toxicology (Waters et al., 2003; Heijne et al., 2005; NRC, 2007), and to an increase of pressure from society and legislation to avoid animal testing.

ITS assumes that a combination of techniques can be able to assess the toxicity of a certain compound replacing, or at least reducing considerably, the need for the use of animals. These techniques should include (DeJongh et al., 1999; Gubbels-van Hal et al., 2005) read-across, chemical categories, (quantitative) structure activity relationships ((Q)SAR), physiologically based pharmacokinetic models (PBPK) and *in vitro* assays. In addition, it is now becoming widely accepted that to progress on our understanding on the toxic effects we must try to understand the toxic mechanism at a molecular level and how molecular changes relate to functional changes at higher levels of biological organization (U.S. EPA, 2003). Recently, the research area devoted to the understanding of the distribution of chemicals at the subcellular level of biosystems, in terms of their properties has been called SBSP - structure-based subcellular pharmacokinetics- (Balaz, 2009). Finally, the incorporation of new functional genomics technologies in toxicology, such as the measurement of gene expression (transcriptomics), protein levels (proteomics) or metabolite contents (metabolomics), should be also considered when developing ITS.

The first attempts to assess the applicability of ITS for the safety evaluation of chemicals (DeJongh et al., 1999; Gubbels-van Hal et al., 2005) were based on the following elements:

- *in vitro*/ QSAR data on ADME (Absorption, Distribution, Metabolism, Excretion) as input data to

- PBPK modelling (rat, human, etc.) for calculating target tissue concentration *in vivo* for the prediction of dose-response curves, NOEL (Not Observed Effect Level), LOEL (Lowest Observed Effect Level), etc.

- *in vitro* and *in vivo* studies to validate the approach.

The application of this approach to a reduced set of substances (ten) to REACH requirements at production levels > ten tonnes shown that it was possible to reduce by 38% the number of animals used, but further improvement was foreseen with the refinement of the procedure (Gubbels-van Hal et al., 2005).

Concerning *in vitro* tests the suggested refinements (Gubbels-van Hal et al., 2005) in the ITS included the need to estimate the partitioning and bioavailability of the chemical in the assay to improve the methodology used to relate *in vitro* toxic concentrations to *in vivo* target tissue concentrations.

An *in vitro* cell-based assay at the HTS (High Throughput Screening) facility (Bouhifd et al., 2008) consists on the use of plastic tissue culture plates with 96 wells where a monolayer of cells in a culture medium with serum is placed and then exposed to the selected dissolved chemicals at several concentration levels. Even though *in vitro* assays are becoming essential to elucidate the toxic potential of chemicals; to analyze the toxic mechanism and the mode of action; and, to replace and to reduce the number of animals; there are still several problems to be solved. Between them the large inter-assay variability, the low sensitivity and the differences found between *in vitro* and *in vivo* experiments in terms of false positives and negatives (Höfer et al., 2004; Lilienblum et al., 2008).

There are several concerns when analyzing the data from *in vitro* experiments. One aspect is the partitioning of organic compounds between the medium, the cells and the container (Blaise et al., 1986). For example, Hestermann et al. (2000) found that up to 56% of 2,3,7,8-tetrachlorodibenzo-p-dioxin was associated with the polystyrene wells. Another aspect is the evaporation of volatile substances and the possibility to cross contamination in adjacent wells as pointed out by Eisentraeger et al. (2003) since test are not performed in sealed wells and the volume to surface ratio is small. Thellen et al. (1989) found this effect for phenol on an algal growth test in a 96 well microplate. Finally, organic substances might not be stable and decompose during the experiment as already pointed out and investigated by Simpson et al. (2003). However, this is a general aspect of organic compounds not only specific of *in vitro* tests. Considering all these aspects, Riedl and Altenburger (2007) concluded that chemicals with an octanol-water partition coefficient, log K_{OW}, higher than 3 and air water partition coefficient, log K_{GL}, higher than -4 would produce less reliable results for algal test toxicity in a microplate assay that in a growth inhibition test conducted in air tight glass vessels.

One possible improvement, already suggested and demonstrated by several research groups (Gülden and Seibert, 2003; Heringa et al., 2004; DeBruyn and Gobas, 2007; Kramer 2010), would be to correct *in vitro* experiments by considering properly the toxic (bioavailable) concentration in the medium which corresponds to the free dissolved concentration. Even though this approach, the partitioning approach (Schwarzenbach et al., 2003), has been largely developed when dealing with fate and distribution of contaminants in the environment (Carafa et al., 2006; Jurado et al., 2007; Dueri et al., 2008; Dueri et al., 2009; Marinov et al., 2009), there have been less work at the level of *in vitro* characterization and modelling.

An aspect as important as the partitioning of the chemical in the cell-based assay is the dynamics of the cells during the experiment. The fundamental process is the expansion of the population of cells due to their growth and division. These processes have also a considerable impact of the cell internal

concentration of the chemical which will change during the experiment and therefore on the toxic effects experienced by the cells. Whereas growth may be seen as a dilution process, cell division will split the chemical content into two cells producing a step change.

In this work, we are developing an integrated modelling approach to improve the characterization and analysis of cell-based assays data. In this first report a mass balance model of the compound based on its physico-chemical properties and the partitioning approach has been implemented and tested. The results have shown the dependence of the dissolved concentration on the physico-chemical properties of the compound and how the value changes over time. In addition, the importance of the partitioning of the chemical into different compartments has been quantitatively assessed.

In the second part of this work a cell development/division model using a bioenergetic modelling approach (DEB, Dynamic Energy Budget) will be developed. Both models will then be coupled with a toxicity and effect model that simulates the uptake and depuration of the toxicant as well as the toxic effects on survival. Furthermore, by combining the results with a PBPK model *in vitro* and *in vivo* concentrations can be compared on equal basis which would produce a better understanding on the toxic potency of a chemical. In addition, this approach will also allow calculating chemical cell internal concentrations and to link the values obtained with the TTC (Thresholds of Toxicological Concern) concept application (Gross et al., 2010).

2. METHODS AND APPROACH

Normally dose-response curves in *in vitro* experiments are represented using the total amount of substance added and not the dissolved (free) concentration which is the bioavailable fraction able to produce a toxic effect. Therefore, *in vitro* dose response curves (or their potency data e.g. EC_{50}, IC_{50} values) does not properly reflect the real toxic potency of a chemical since the compound will partition into the medium dissolved organic and particulate organic carbon (mainly serum and cells), and into the plastic walls as well as into the headspace (Gülden at al., 2001; Heringa et al., 2004; amongst others). Another aspect that should be considered when volatile compounds are tested is the possibility of evaporation and cross contamination.

In addition, during the experiments cells growth and divide consuming nutrients, therefore the partitioning characteristic of the medium changes with time as well as the internal concentrations in the cells complicating even further the comparison between different *in vitro* experiments and systems and therefore call for an integrated modelling approach able to quantify all this aspects and to "correct" the nominal concentrations as a function of the cell-based assay and the physico-chemical properties of the tested compounds. Part of this integrated modelling approach must be:

- Fate and transport model
- Growth and division model

- Toxicodynamics model

The solution of the ordinary differential equations of the model should allow the calculation over time of the dissolved concentration of a chemical as well as the internal concentration in the cell-based assay. We are briefly going to illustrate the different models and how they are interrelated.

In this first work, we will develop and test the fate and transport model, whereas in the second part the growth and toxicodynamics models will be developed and validated.

2.1. FATE AND TRANSPORT: MASS BALANCE MODEL

The fate and transport model consists of a dynamic mass balance that includes a time-variable chemical transport and fate model for calculating the chemical concentration in the medium as well as in the headspace. The gas phase has been included to consider, in a second step, the possible losses and cross contamination between the 96 wells in the TC plates, since the TC are not hermetic even though the system was designed to minimize this aspect. To quantify this phenomenon, there are not enough experimental data at the moment.
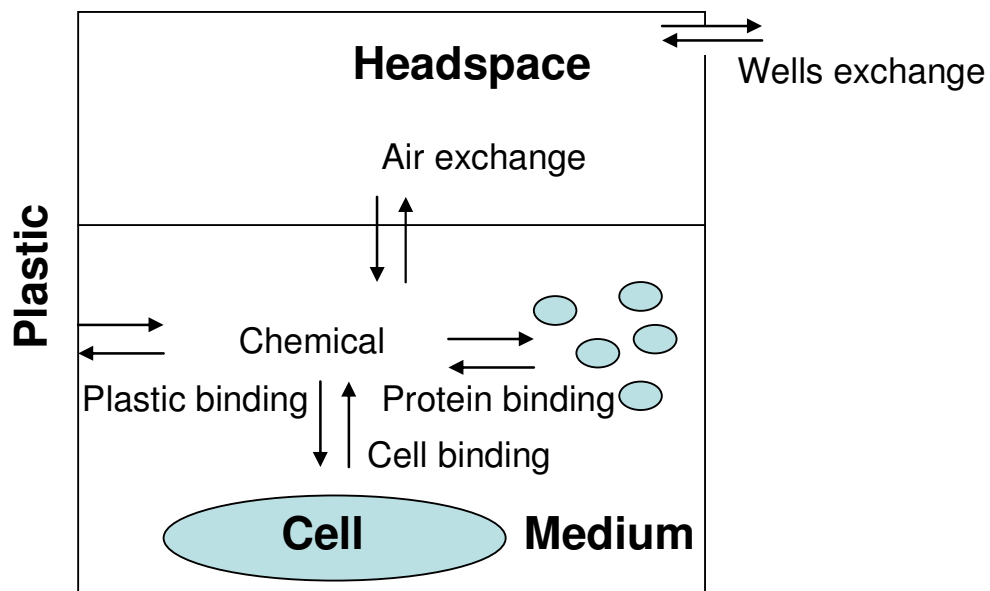

Figure 1. Overview of the process included in the fate and transport model (modified from Kramer, 2010)

Assuming a well mixed medium and headspace and that the sorption processes are fast compared with the other processes then the mass balance equations for both compartments can be written as:

- *Total concentration in the medium*:

$$V_M \frac{dC_T}{dt} = A_s \cdot F_{AW} - k \cdot V_M \cdot C^{diss} \tag{1}$$

where V_M refers to the volume of the medium (m^3) and T refers to the total concentration (mg m^{-3}); the first term of the rhs represent the transfer of chemical across the air-water interface whereas the second term represent transformation/losses from the medium, e.g. degradation, decomposition, etc.

- Total concentration in the air:

A similar equation can be written for the headspace:

$$V_H \frac{dC^{Air}}{dt} = -A_s \cdot F_{AW} - A_l \cdot F_l \tag{2}$$

where V_H refers to the headspace volume (m^3); the first term represents the transfer of chemical across the air-water interface whereas the second term represents the losses from the headspace due to gas exchange, which we will consider zero in this first approach.

To model the partitioning of an organic chemical in the medium (Kramer, 2010), we can consider that the compounds are either purely dissolved (C^{diss}), bound to the serum in the culture medium (C^S), bound to the cells (C^{cell}) and bound to the (plastic/glass) surface of the culture vessel (C^p). Therefore, the total concentration of an organic contaminant in the medium, C^T, can be described by following equation:

$$C^T = C^{diss} + C^S + C^{cell} + C^p \frac{S_M}{V_M} \tag{3}$$

where S_M refers to the surface of the well in contact with the medium.

2.1. 1. Partitioning of chemicals

A general approach to describe the distribution of the organic compound is by means of the partition coefficients K_i, defined as the relationships between the concentration in a particular medium and in the water. In this case we need to calculate:

- <u>Serum protein partitioning</u>:

$$K_S = \frac{C^S/[S]}{C^{diss}} \tag{4}$$

where [S] is the concentration of proteins in the medium (mole protein·m^{-3}). Kramer (2010) found the following correlation studying PAHs:

$$\log K_S = 0.37(\pm 0.03)\log K_{ow} - 0.29(\pm 0.12) \tag{5}$$

where the partition coefficient K_S is expressed in m^3·mol^{-1}. A MW = 66400 g/mol is used for Bovine Serum Albumin (BSA). In a compilation of blood protein (albumin) data DeBruyn and Gobas (2007) for different tissues found that the sorptive capacity of protein in solid animal tissues was higher than K_{ow} for low K_{ow} chemicals (-1.3$\leq$ log K_{ow} $\leq$2) with a value around 1.31($\pm$0.62) (ml g^{-1} albumin). For more lipophobic chemicals (2 < log K_{ow} ≤ 5.1) the logarithm of the partition constant increased with log K_{ow} following: 0.57 log K_{ow} +0.69, whereas at higher K_{ow} approached the lipid equivalence value

of 0.05, i.e. log K_{ow}-1.3. In addition, they recommended, for modelling purposes, to estimate the sorptive capacity of animal protein as 5% that of lipid.

Normally, these correlations refer to non-specific binding. Depending on the specific structure of the chemical and the protein, specific binding can occur and then the value could be completely different.

- Partitioning to well plate plastic:

The partitioning constant to plastic, K_p (m), is defined as:

$$K_p = \frac{C^p}{C^{diss}} \qquad (6)$$

where C^p (mg m^{-2}) is the concentration sorbed in plastic. Kramer (2010) found a linear correlation between K_p and K_{ow} for the PAHs (Polycyclic aromatic hydrocarbons) family.

$$\log K_p = 0.97(\pm 0.15)\log K_{ow} - 6.94(\pm 0.80) \qquad (7)$$

As an example, if we consider a well with half of the liquid and a hydrophobic compound such as Benzo[a]pyrene (log K_{ow} = 6.13 and log K_p = -0.99), 98% of Benzo[a]pyrene binds to plastic.

- Partitioning to cells:

According to Kramer (2010) the partition coefficient of a chemical with cells, K_C (m^3 kg^{-1}), could be equated to their partition with the lipid content, K_{lip}, and therefore it was possible to write:

$$K_C = \frac{C^{cell}/[C]}{C^{diss}} \qquad (8)$$

where $[C]$ is the concentration of cell lipid in medium (kg m^{-3}). Jonker and van der Heijden (2007) found for PAHs a linear correlation between the lipid-water partition coefficient and the octanol water partition coefficient as:

$$\log K_C = 1.25(\pm 0.06)\log K_{ow} - 3.70(\pm 0.37) \qquad (9)$$

The relationship between the concentration in an organism (the cell) and in the water is called the bioconcentration factor (BCF). It has been demonstrated (Swackhamer and Skoglund, 1993; Stange and Swackhamer, 1994) that, for many organic compounds, the logarithm of the bioconcentration factor plotted against the logarithm of the octanol/water partition coefficient gives two linear correlations (with a plateau in correspondence to log $K_{ow} \approx$ 6.5, that can be fitted by least squares and may be represented by the following log linear equations (Del Vento and Dachs, 2002):

log BCF= 1.085 log K_{ow} – 3.770   for log K_{ow} < 6.4   (10)

log BCF= 0.343 log K_{ow} + 0.913   for log $K_{ow} \geq$ 6.4   (11)

BCF is expressed in m^3 kg^{-1}.

The existence of this plateau has been questioned by Jonker and van der Heijden (2007) due to two factors: equilibrium was not reached when the measurement was done and the dissolved organic carbon (DOC) concentration was not considered in the measurement.

All these relationships presuppose that the compound has a linear sorption isotherm which is normally a good approximation at low concentrations. In addition, it is also assumed that there is no saturation (plastic surface, protein binding sites, etc.) which may occur in experiments at high doses. Even though the correlations are probably only valid for PAHs, in this work we will use it as a first approximation to develop the model and then we will test the results for other families of compounds using literature data.

The partition of the compound between the different phases can be expressed as a function of the total (nominal) concentration in the well as:

$$C^{diss} = \frac{C_T}{1 + K_S \cdot [S] + K_C \cdot [C] + K_p \cdot \dfrac{S_M}{V_M}} \tag{12}$$

$$C^{S} = \frac{K_S \cdot [S] \cdot C_T}{1 + K_S \cdot [S] + K_C \cdot [C] + K_p \cdot \dfrac{S_M}{V_M}} \tag{13}$$

$$C^{cell} = \frac{K_C \cdot [C] \cdot C_T}{1 + K_S \cdot [S] + K_C \cdot [C] + K_p \cdot \dfrac{S_M}{V_M}} \tag{14}$$

$$C^{P} = \frac{K_P \cdot C_T}{1 + K_S \cdot [S] + K_C \cdot [C] + K_p \cdot \dfrac{S_M}{V_M}} \tag{15}$$

2. 1. 2. Air-Water Exchange

Organic pollutants will move in the headspace of the well and since the TC plates are not hermetically close they will diffuse to the other wells during the experiment. The final concentration will depend on the physico-chemical properties of the assessed compound as well as on the dosed concentrations. As a first approximation, we will concentrate on simulating the air-water exchange on a well assuming no transport outside takes place, but we will write the mass balance equation and, when experimental data will become available, we will be able to model the diffusion to other wells in the plate. In this case, the exchange between the headspace and the aqueous medium occurs through diffusive gas exchange between the headspace and medium boundary layer.

- Diffusive exchange

The diffusive air-water exchange flux F_{AW} at the interface (*i*) is represented as (Westerterp et al., 1984):

$$F_{AW} = k_{AW}\left(\frac{C^{air}}{K_{GL}} - C^{diss}\right) \tag{16}$$

where C^{air} and C^{diss} are the gas-phase and the dissolved (liquid) concentrations, respectively. K_{GL} is the dimensionless gas-liquid distribution coefficient, $K_{GL} = C_G^i / C_L^i$, and is calculated from the Henry's law constant using:

$$K_{GL} = \frac{H}{R \cdot T} \tag{17}$$

where H (Pa m^3 mol^{-1}) is the Henry law constant, R is the universal gas constant, 8.314 J·(mol·K)$^{-1}$, and T is the temperature (K). The temperature dependence of Henry's law constant can be expressed as:

$$\ln H = A_H + \frac{B_H}{T} \tag{18}$$

where A_H and B_H are two constants that depend on the specific compound.

The mass transfer coefficient k_{AW} is given by following equation:

$$k_{AW} = \left(\frac{1}{k_G \cdot K_{GL}} + \frac{1}{k_L}\right)^{-1} \tag{19}$$

where and k_G and k_L are the mass transfer coefficients (m s^{-1}) in the air and the water films, respectively.

The liquid phase mass transfer coefficient, k_L, is calculated from the mass transfer coefficient of CO_2 in the water side, k_{LCO_2} (Kanwisher, 1963) which when there is no wind has a constant value: $k_{LCO_2} = 4.1 \cdot 10^{-2}$ (m s^{-1}), by applying a correction factor:

$$k_L = k_{LCO_2}\left(\frac{Sc}{600}\right)^{-0.5} \tag{20}$$

where Sc is the Schmidt number of the pollutant and 600 accounts for the Schmidt number of CO_2 at 298 K. The Schmidt number is defined as:

$$Sc = \frac{\mu}{D_L \cdot \rho} \tag{21}$$

where ρ and μ are the density and viscosity of the fluid respectively while D_L is the coefficient of molecular diffusion of the dissolved compound. The temperature dependence of the diffusion coefficient in water is calculated with following correlation by Wilke and Chang (1955):

$$D_L = \frac{7.4 \cdot 10^{-12} (\alpha MW)^{0.5}}{\mu \cdot V_b^{0.6}} \cdot T \tag{22}$$

8

where T is the temperature of the solvent [K] and μ is its viscosity [cP], V_b [cm^3 mol^{-1}] is the molar volume of the organic compound at its normal boiling point, MW is the molecular weight [g mol^{-1}] of solvent and α is the association factor of the solvent, $\alpha = 2.6$ for organic solutes diffusing into water (Perry and Chilton, 1984) and D_L is given in m^2 s^{-1}.

The gas phase mass transfer coefficient, k_G, is calculated using the mass transfer coefficient for water, which for the case of no wind has a constant value: $k_{G,H_2O} = 3 \cdot 10^{-3}$ (m·s^{-1}), and then

$$k_G = k_{G,H_2O} \left(\frac{D_G}{D_{G,H_2O}} \right)^{0.67} \tag{23}$$

where D_G and $D_{G,H2O}$ refers to the diffusion coefficients in the gas phase (air) of the chemical and water, respectively (Schwarzenbach et al., 2003).

An empirical correlation that has been extensively used to estimate the diffusion coefficients in air, D_G in m^2 s^{-1}, as a function of temperature is the one presented in Fuller et al. (1966):

$$D_G = \frac{10^{-7} \cdot T^{1.75} \left(\dfrac{MW_{Air} + MW_B}{MW_{Air} \cdot MW_B} \right)^{1/2}}{P \left(\left[\sum (\upsilon)_{Air} \right]^{1/3} + \left[\sum (\upsilon)_B \right]^{1/3} \right)^2} \tag{24}$$

where T is the temperature (K), P is the pressure (atm), MW are the molecular weights (g/mol) of air (28.8) and the organic compound, and υ are the atomic diffusion values, $\Sigma\upsilon_{Air}$=20.1, that can be determined form the values in Table 1.

Table 1. Atomic diffusion volumes for use in estimating D by the method of Fuller, Schettler and Giddings (1966).

C	16.5	Cl	19.5
H	1.98	S	17.0
O	5.48	Aromatic ring	-20.2
N	5.69	Heterocyclic ring	-20.2

For the specific case of water in air, which is used after to calculate the mass transfer coefficient in the gas phase, we have adjusted the experimental values modifying the atomic diffusion values, i.e. $\Sigma\upsilon_{water}$=10.8., then the diffusion coefficient of water in air is calculated as:

$$D_{G,H_2O} = 1.2365 \cdot 10^{-9} T^{1.75} \tag{25}$$

2.1.3. Degradation, Decomposition and Metabolism

In absence of detailed experimental data, degradation, decomposition or metabolism fluxes are represented as a first order reaction model. Therefore for degradation and decomposition we will have:

$$F_{\deg r} = k_{\deg r} \cdot C^{diss} \tag{26}$$

where C^{diss} is the concentration of the contaminant in dissolved form and k_{degr} may be the degradation rate resulting from hydrolysis, photodegradation, etc. Normally, when no detailed data is available, the degradation rate k_{degr} is calculated from half life times

$$t_{1/2} = \frac{\ln 2}{k_{\deg r}} \tag{27}$$

For metabolism, we will assume the same principle and write:

$$F_{met} = k_{met} \cdot C^{cell} \tag{28}$$

Then, the metabolism rate will be obtained from biodegradation half-times as above.

2.2. EXPERIMENTAL SET-UP AND CELL LINE CHARACTERISTICS

The experimental procedure for the 3T3 BALB/c Neutral Red Uptake (NRU) cytotoxicity assay was developed for the NICEATM/ECVAM validations study requirements (ICCVAM, 2006a, b), whereas issues concerning the automation and the implementation of the assay using the Pilot Test Platform (PTP) of the IHCP automated test facility may be found in Bouhifd et al. (2005) and Bouhifd and Whelan (2006).

The results of the testing for the validation study have been reported in ICCVAM (2006a) whereas the results obtained by testing 28 chemicals at the High Throughput Screening (HTS) platform are described in Norlén et al. (2007).

The configuration of the 96-well test plate is shown in Fig.2. The dimensions of each well are:

- Top internal radius: $3.425 \cdot 10^{-3}$ m.

- Bottom internal diameter: $3.175 \cdot 10^{-3}$ m.

- Depth: $10.76 \cdot 10^{-3}$ m.
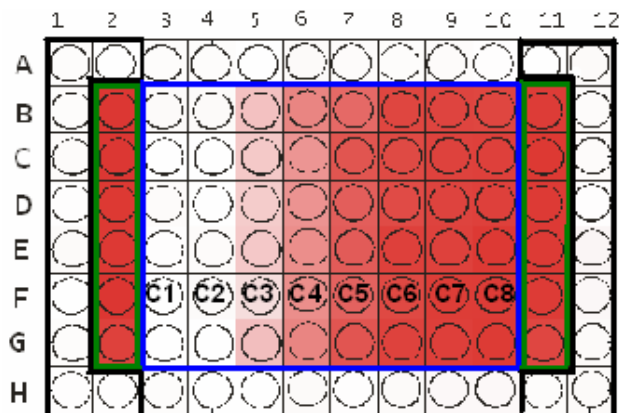
- Bottom area $3.16 \cdot 10^{-5}$ m^2

Figure 2. Configuration of the 96-well test plate. Blue: cells with dosing solutions of test chemical, six replicates for each dose and eight concentrations, C1 is the highest and C8 is the lowest concentration; green: Black: only medium, blank experiments; green: Vehicle Controls (VC), contain cells in medium and no test compound (the VCs are considered to have 100% viability).

With these dimensions and assuming the experiments contained 100 μL, i.e. $V_M = 10^{-7}$ m^3, we can obtain:

- Total well volume (assuming a truncated cone):

$$V_W = \frac{1}{3}\pi\left(r^2 + r \cdot R + R^2\right)h = 3.683 \cdot 10^{-7} \text{ m}^3.$$

- Headspace volume (m^3): $V_H = 2.683 \cdot 10^{-7}$ m^3.

- Surface of the well in contact with the medium, $S_M = \pi(r + r_m)g + S_{bottom}$, where r_m is the radius of the occupied volume and g is the slant height. $S_M = 9.392 \cdot 10^{-5}$ m^2.

- Surface of the cell-based assay medium, $A_S = \pi \cdot r_m^2 = 3.312 \cdot 10^{-5}$ m^2.

Assuming a 5% (v/v) serum in the medium, then $[S]_0 = 2.34\ 10^{-2}$ mol protein m^{-3}.

For 3T3 cells, a volume of $1.8 \pm 0.7\ 10^{-15}$ m^3/cell was calculated by Gülden et al. (2002), considering spherical cells. Also the protein content was assessed, with 0.37 ± 0.11 mg/10^6 cells with a ratio of 0.231 mg lipid/mg protein. A doubling time of ~19 h was measured in the HTS laboratory[1], see Fig. 3. Assuming an initial concentration of $2.0 \cdot 10^3$ cells at each well, we can calculate the number of cells as a function of time as: $n_{cells} = 2.0 \cdot 10^3 \cdot \exp(1.0098 \cdot 10^{-5} \cdot t)$, where t is the time in s from the beginning of the experiment. Therefore: $[C] = 1.1877 \cdot 10^{-6} \cdot n_{cells}$ (kg lipids m^{-3}).
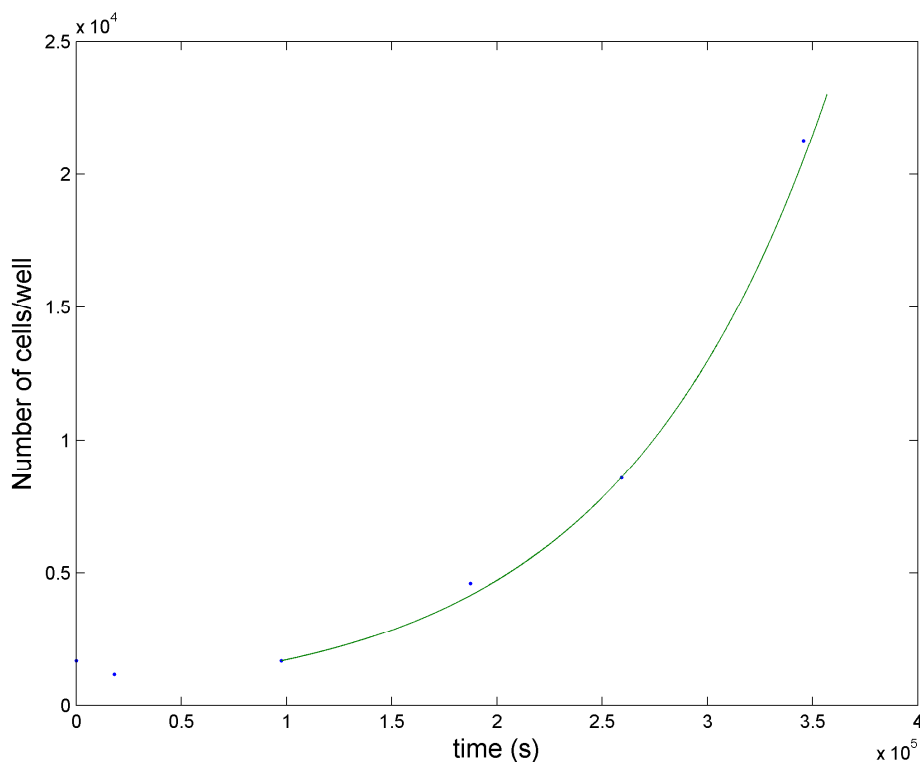

Figure 3. Experimental measured growth of 3T3 cells and fitted exponential curve after acclimatization.

---

[1] In the second report a model for growth and reproduction will be added that will replace this part.

The total cell volume changes between $3.74 \cdot 10^{-12}$ m^3 and $2.14 \cdot 10^{-11}$ m^3 which represent the 0.0037 and the 0.021% of the total volume. Therefore we can neglect this change when compared with the medium volume.

3. RESULTS

3.1. SIMULATION OF PAHs DISTRIBUTION

Since some of the partitioning coefficients developed by Kramer (2010) were experimentally verified for Polycyclic Aromatic Hydrocarbons (PAH), we will first test here the simulation results for this family of compounds. The differences between our approach and the approach developed by Kramer (2010) resides mainly in the dynamic aspect of our simulation and in our objectives toward an integrated modelling approach, including the cell growth and reproduction model and toxicodynamics as a function of internal concentrations in the cell, which will constitute the second part of this report.
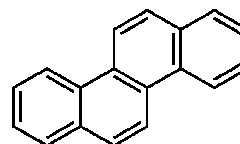
Polycyclic aromatic Hydrocarbons are produced during combustion of carbonaceous materials including wood and fuel oils, especially under limited oxygen availability. They are also emitted during aluminium smelting. There are several natural and anthropogenic sources for these compounds. Furthermore, there is a growing concern because several of them are believed to be human carcinogens, mutagenic and teratogenic (IARC, 1991).

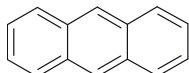In this report, we have selected twelve PAHs to simulate. These are:
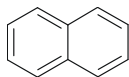
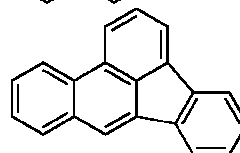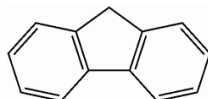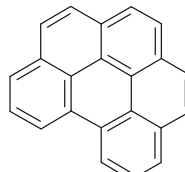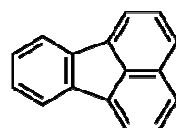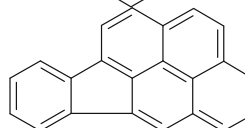|			
Naphthalene		Chrysene	
Anthracene		Benzo [b] fluoranthene	
Fluorene		Benzo [k] fluoranthene	
Phenanthrene		Benzo [a] pyrene	
Pyrene		Benzo [ghi] perylene	
Fluoranthene		Indeno [1,2,3,cd] pyrene	
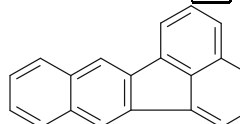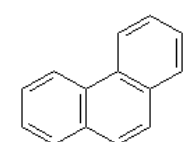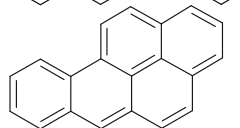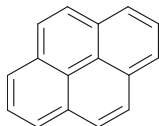
The physico-chemical parameters for the PAHs family, as well as literature references are given in Table 2.

Table 2. Specific PAHs parameters.

Parameter		Range			Ref
MW	Molecular weight (g/mol)	128.17	:Naphthalene		
		178.23	:Anthracene		
		166.22	:Fluorene		
		178.23	:Phenanthrene		
		202.26	:Pyrene		
		202.26	:Fluoranthene		
		228.30	:Chrysene		
		252.29	:Benzo [b] fluoranthene		
		252.29	:Benzo [k] fluoranthene		
		252.29	:Benzo [a] pyrene		
		276.31	:Benzo [ghi] perylene		
		276.31	:Indeno [1,2,3-cd] pyrene		
MV	Molar volume (cm^3/mol)	148.0	:Naphthalene		
		197.0	:Anthracene		
		188.0	:Fluorene		
		199.0	:Phenanthrene		
		214.0	:Pyrene		
		217.0	:Fluoranthene		
		251.0	:Chrysene		
		253.0	:Benzo [b] fluoranthene		
		253.0	:Benzo [k] fluoranthene		
		263.0	:Benzo [a] pyrene		
		277.0	:Benzo [ghi] perylene		
		265.8	:Indeno [1,2,3-cd] pyrene		
H	Henry (Pa m^3/mol) values $\ln H = A_h - B_h/T$	A_h	B_h		Paasivirta et al. 1999; Bamford et al. 1999.
		5.07	922	:Naphthalene	
		21.91	6013	:Anthracene	
		22.52	6044	:Fluorene	
		21.31	5925	:Phenanthrene	
		17.57	5104	:Pyrene	
		17.26	4946	:Fluoranthene	
		42.05	12727	:Chrysene	
		9.83	3275	:Benzo [b] fluoranthene	
		9.83	2979	:Benzo [k] fluoranthene	
		12.02	3558	:Benzo [a] pyrene	
		12.83	4006	:Benzo [ghi] perylene	
		10.36	3208	:Indeno [1,2,3-cd] pyrene	
K_{ow} (298 K)	Octanol-water partition coefficient	$2.34 \cdot 10^3$	:Naphthalene		Mackay and Hickie 2000
		$3.47 \cdot 10^4$	:Anthracene		
		$1.32 \cdot 10^4$	:Fluorene		
		$3.73 \cdot 10^4$	:Phenanthrene		
		$1.51 \cdot 10^5$	:Pyrene		
		$1.70 \cdot 10^5$	:Fluoranthene		
		$6.46 \cdot 10^5$	:Chrysene		
		$2.75 \cdot 10^6$	:Benzo [b] fluoranthene		
		$2.75 \cdot 10^6$	:Benzo [k] fluoranthene		
		$1.10 \cdot 10^6$	:Benzo [a] pyrene		
		$7.94 \cdot 10^6$	:Benzo [ghi] perylene		
		$3.84 \cdot 10^6$	:Indeno [1,2,3-cd] pyrene		
k_{deg}	Decomposition rate in water column (s^{-1})]	$6.7 \cdot 10^{-7}$	:Naphthalene		Mackay and Hickie 2000
		$3.5 \cdot 10^{-7}$	:Anthracene		
		$3.8 \cdot 10^{-7}$	:Fluorene		
		$1.1 \cdot 10^{-7}$	:Phenanthrene		
		$1.1 \cdot 10^{-7}$	:Pyrene		
		$1.1 \cdot 10^{-7}$	:Fluoranthene		
		$1.1 \cdot 10^{-7}$	:Chrysene		
		$3.5 \cdot 10^{-7}$	:Benzo [b] fluoranthene		
		$3.5 \cdot 10^{-7}$	:Benzo [k] fluoranthene		
		$1.1 \cdot 10^{-7}$	:Benzo [a] pyrene		
		$1.3 \cdot 10^{-8}$	:Benzo [ghi] perylene		
		$1.3 \cdot 10^{-8}$	:Indeno [1,2,3-cd] pyrene		

The dynamical system, Eqs. (1)-(2) was run for the twelve PAHs for 48 h assuming there was no decomposition, the serum concentration was constant and there were no toxicity effects, i.e. the cell growth was equivalent in all experiments. As an example, Figures 4 and 5 show the variation in the total concentration in the medium and in the headspace as a function of time for results for Naphthalene and Indeno[1,2,3-cd]pyrene, whereas Figures 6 and 7 show the variation of the distribution of the concentration in the medium for the same compounds. Finally, Table 3 summarizes the partitioning (in percentages) for all compounds at the end of the simulation, i.e. after 48 h.
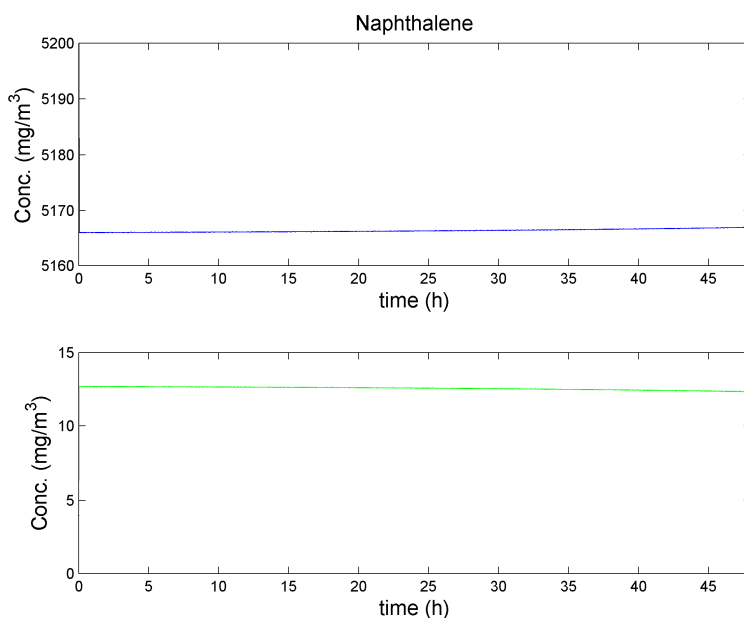

Figure 4. Simulated Naphthalene total concentration in the medium (top) and in the headspace (bottom).
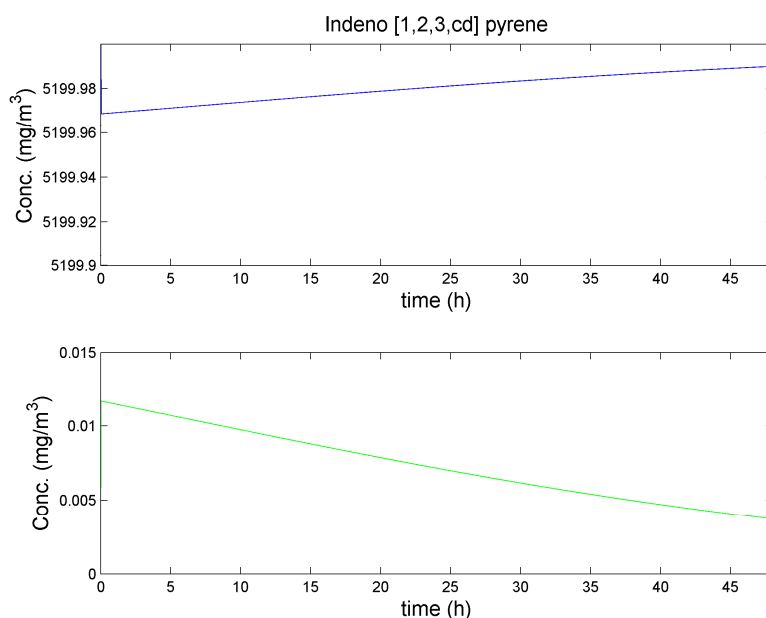

Figure 5. Simulated Indeno [1,2,3,cd] pyrene total concentration in the medium (top) and in the headspace (bottom).
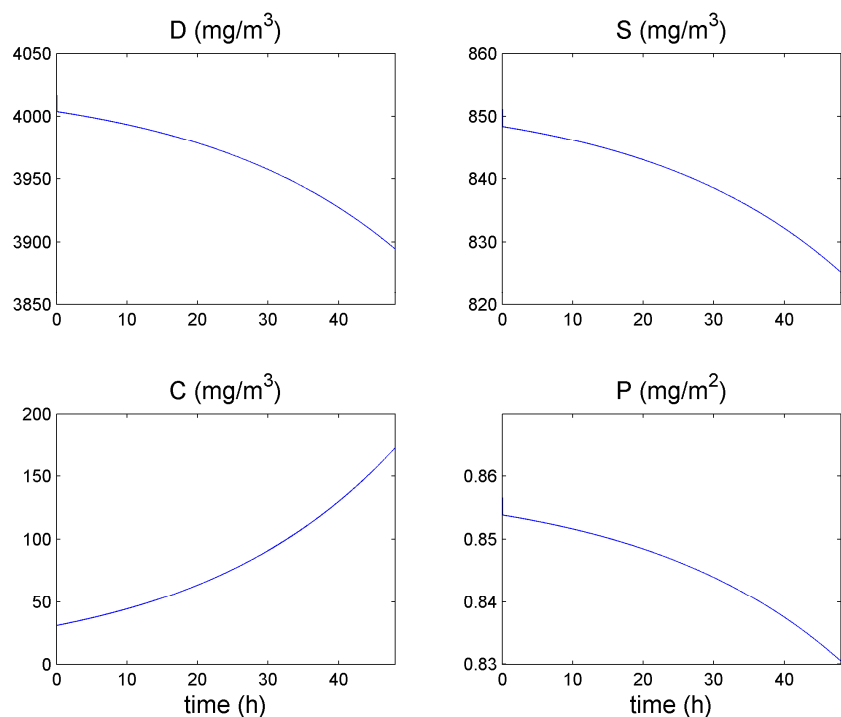
14

Figure 6. Simulated Naphthalene concentrations in the dissolved phase (D), bound to the serum (S), attached to the cells (C) and to the plastic surface in contact with the medium (P).
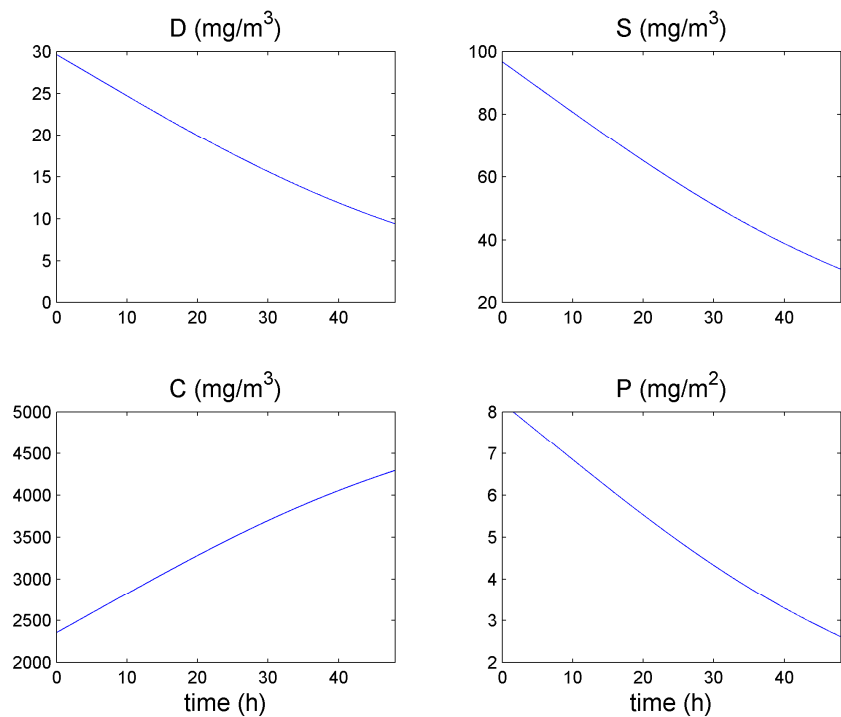

Figure 7. Simulated Indeno [1,2,3,cd] pyrene concentrations in the dissolved phase (D), bound to the serum (S), attached to the cells (C) and to the plastic surface in contact with the medium (P).

15

Table 3. Final distribution in mass percentages of the PAHs between headspace (H), and medium: dissolved (D), serum (S), attached to cells (C) and to the plastic wall (P).

Compound	H	D	S	C	P
Naphthalene	0.63	74.89	15.87	3.32	5.29
Anthracene	0.34	26.08	14.97	33.48	25.13
Fluorene	0.99	45.80	18.39	17.56	17.27
Phenanthrene	0.23	24.82	14.62	34.75	25.58
Pyrene	0.022	7.08	7.01	57.38	28.50
Fluoranthene	0.024	6.29	6.50	58.87	28.31
Chrysene	0.0042	1.45	2.46	72.19	23.89
Benzo [b] fluoranthene	0.0001	0.27	0.77	81.09	17.88
Benzo [k] fluoranthene	0.0003	0.27	0.77	81.09	17.88
Benzo [a] pyrene	0.0014	0.79	1.62	75.92	21.66
Benzo [ghi] perylene	0.0001	0.07	0.32	85.58	14.03
Indeno [1,2,3,cd] pyrene	0.0002	0.18	0.59	82.59	16.64

During the previous simulations we did not consider decomposition reactions taking place. Assuming that the water environmental half-life times provided by Mackay and Hickie (2000) are realistic for an *in vitro* experiment, we have checked if there are differences in the simulated results. As an example, Figures 8 and 9 show the comparison of the results without and with the decomposition reaction. As can be observed there are substantial differences between both cases.
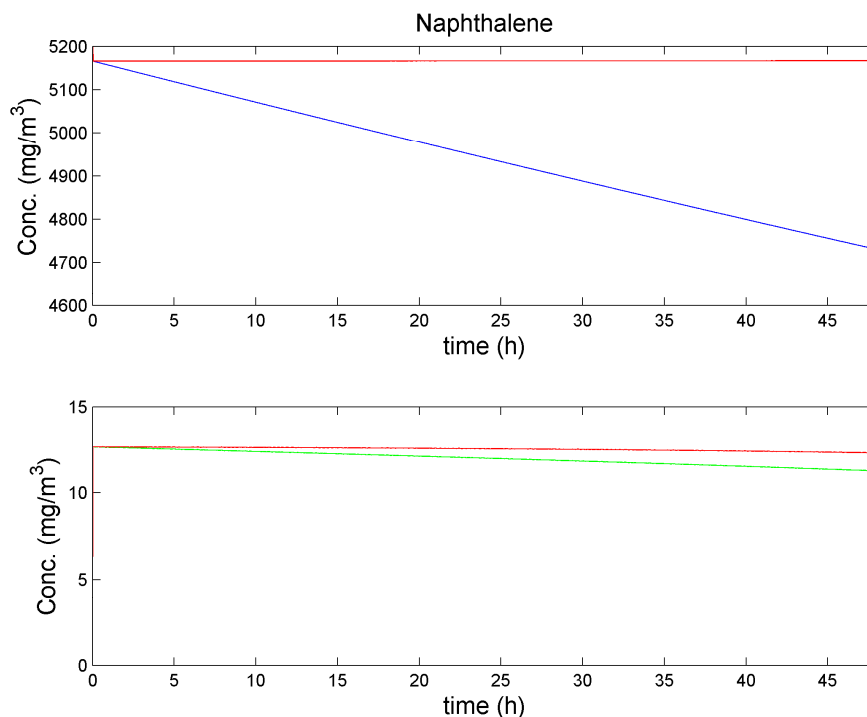

Figure 8. Simulated Naphthalene total concentration in the medium (top) and in the headspace (bottom) without decomposition (red lines) and with decomposition reaction.
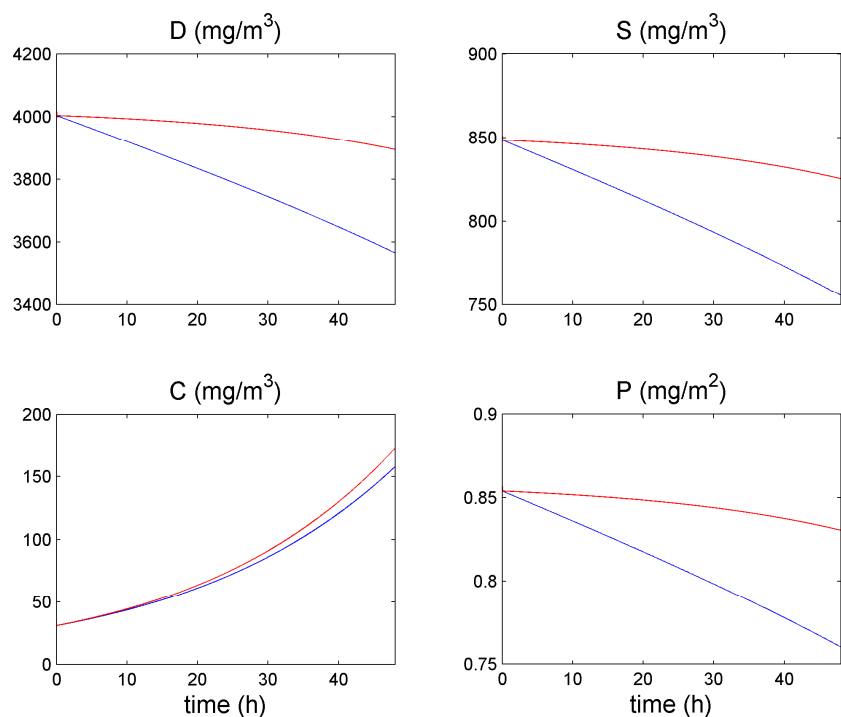
16

Figure 9. Simulated Naphthalene concentrations in the dissolved phase (D), bound to the serum (S), attached to the cells (C) and to the plastic surface in contact with the medium (P) without decomposition (red lines) and with decomposition reaction.

3.2. SIMULATION OF LITERATURE CASE STUDIES

To assess the potential of using the same correlations to calculate the fate of a certain chemical in the cell-based assays, we have run the model trying to simulate experimental from other families of compounds. Therefore, we have applied the modelling approach to data sets corresponding to two different families of compounds: organochlorine pesticides (p,p'-DDT; p,p'-DDE; dieldrin and lindane) and chlorophenols (Pentachlorophenol; 2,4,5-trichlorophenol; 2,4-dichlorophenol; 4-chlorophenol and phenol).
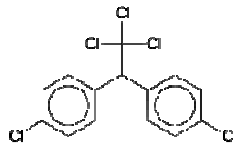
17
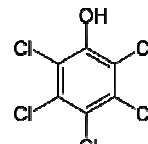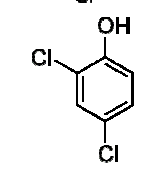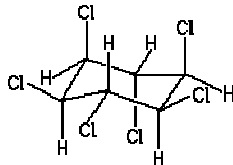
lindane   4-chlorophenol
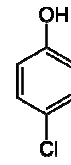
phenol

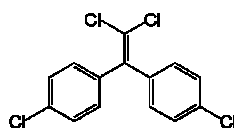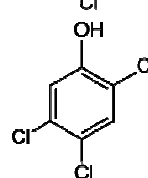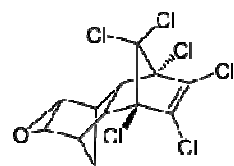Table 4. Specific physico-chemical parameters.

Parameter		Range		Ref
MW	Molecular weight (g/mol)	354.49	: p,p'-DDT	
		318.02	: p,p'-DDE	
		380.91	: dieldrin	
		290.83	: lindane	
		266.34	: Pentachlorophenol	
		197.45	: 2,4,5-trichlorophenol	
		163.00	: 2,4-dichlorophenol	
		128.56	: 4-chlorophenol	
		94.11	: phenol	
MV	Molar volume (cm^3/mol)	335.4	: p,p'-DDT	
		318.0	: p,p'-DDE	
		217.7	: dieldrin	
		135.0	: lindane	
		184.0	: Pentachlorophenol	
		133.0	: 2,4,5-trichlorophenol	
		125.0	: 2,4-dichlorophenol	
		102.0	: 4-chlorophenol	
		88.0	: phenol	
H	Henry (Pa m^3/mol) values $\ln H = A_h - B_h/T$	A_h	B_h	Paasivirta et al. 1999; EPI Suite
		13.02	3369 : p,p'-DDT	
		12.62	3291 : p,p'-DDE	
		11.58	3093 : lindane	
	H (298 K)	1.01	: dieldrin	
		$2.48 \cdot 10^{-3}$	: Pentachlorophenol	
		$1.64 \cdot 10^{-1}$	: 2,4,5-trichlorophenol	
		$4.35 \cdot 10^{-1}$	: 2,4-dichlorophenol	
		$6.35 \cdot 10^{-2}$	: 4-chlorophenol	
		$3.72 \cdot 10^{-2}$	: phenol	
log K_{ow} (298 K)	Octanol-water partition coefficient	6.31	: p,p'-DDT	EPI suite[TM]
		6.96	: p,p'-DDE	
		5.30	: dieldrin	
		3.86	: lindane	
		5.12	: Pentachlorophenol	
		3.72	: 2,4,5-trichlorophenol	
		3.06	: 2,4-dichlorophenol	
		2.39	: 4-chlorophenol	
		1.46	: phenol	
k_{deg}	Decomposition rate in water column (s^{-1})]	$2.44 \cdot 10^{-9}$	: p,p'-DDT	EPI suite[TM]
		$2.55 \cdot 10^{-9}$	: p,p'-DDE	
		$4.46 \cdot 10^{-8}$	: dieldrin	
		$4.46 \cdot 10^{-8}$	: lindane	
		$4.46 \cdot 10^{-8}$	: Pentachlorophenol	
		$1.34 \cdot 10^{-7}$	: 2,4,5-trichlorophenol	
		$2.13 \cdot 10^{-7}$	: 2,4-dichlorophenol	
		$5.34 \cdot 10^{-7}$	: 4-chlorophenol	
		$5.34 \cdot 10^{-7}$	: phenol	

In this case, we have modified the experimental conditions as reported by Gülden et al. (2002): $V_M = 2 \cdot 10^{-7}$ m^3; $n_{cells} = 6.0 \cdot 10^3 \cdot \exp(9.1686 \cdot 10^{-6} \cdot t)$ (~21 h doubling time); duration of the experiment 72 h. The normal culture medium containing $[S]_0 = 1.81 \ 10^{-2}$ mol·protein m^{-3} was supplemented with additional

38.8 mg·ml^{-1} BSA obtaining cultures with $[S]_0=0.602$ mol·protein m^{-3}. Table 5 summarises the results of both simulations and shows the comparison with experimental data from Gülden et al. (2002).

Table 5. Comparison between experimental and calculated fraction attached to serum. Data from Gülden et al. (2002).

Substance	Exp.fraction [S]$_0$=1.81 10^{-2} mol·protein m^{-3}	Calc. fraction	Exp. fraction [S]$_0$=0.602 mol·protein m^{-3}	Calc. fraction
p,p'-DDT	0.075	0.093	0.74	0.77
p,p'-DDE	0.10	0.066	0.79	0.70
dieldrin	0.14	0.15	0.86	0.85
lindane	0.17	0.17	0.87	0.87
Pentachlorophenol	1.00	0.16	1.00	0.86
2,4,5-trichlorophenol	0.68	0.31	0.98	0.94
2,4-dichlorophenol	0.09	0.23	0.77	0.91
4-chlorophenol	0.10	0.12	0.77	0.82
phenol	0.0	0.04	0.0	0.57

4. DISCUSSION

4.1. K_S CORRELATIONS

Figure 10 shows the two correlations used in this work. Whereas Kramer (2010) correlation was developed specifically for PAHs (logK_{ow} between 3.3 and 6.1), the correlation from deBruyn and Gobas (2007) is based on a literature analysis covering a wide margin of log K_{ow} values (-1.3 to 8.8). For the simulation of cell-based assays for PAHs we employed the first correlation, whereas for the simulations in Table 9 (log K_{ow} from 1.5 to 7) we used the second correlation which improved the results when compared with the experimental data.
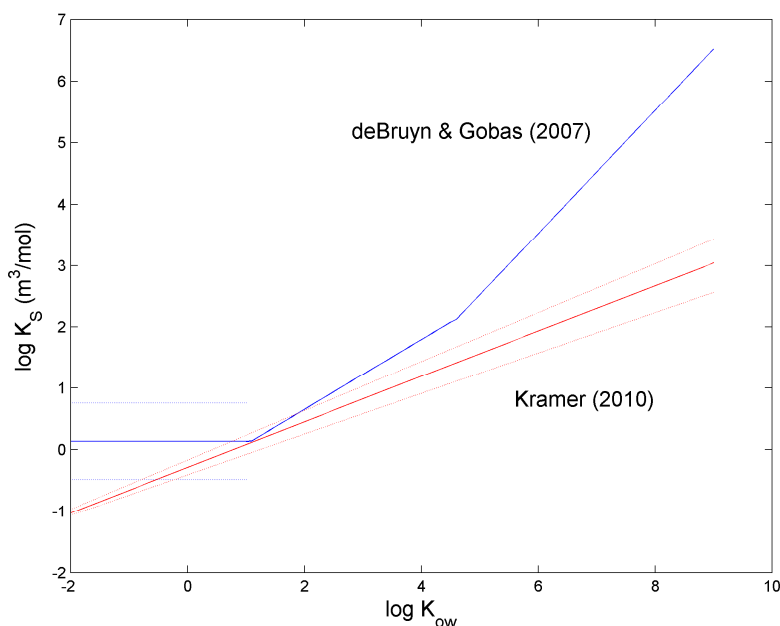

Figure 10.Comparison between the two correlations to calculate K_S as a function of K_{ow} used in this work.

In any case, independently of the correlation used, the results point out the importance to considering the binding to proteins when assessing the toxicity of a certain compound. In addition, they have also shown that there are some problems to characterize this influence by considering only the K_{ow}, see for example the extreme cases, from one to zero, of pentachlorophenol and phenol, but in general terms they probably would improve the assessment of the toxicity of a certain compound.

The case of pentachlorophenol may be due to specific binding with albumin, whereas for phenol, there is a high variability (see confidence intervals in Fig. 10) at log K_{ow} values lower than 2.

4.2. THE INFLUENCE OF SERUM ON *in vitro* EXPERIMENTS

Another aspect to consider is the type of effect serum has on the EC_{50} values obtained during *in vitro* experiments. Gülden et al. (2002) found a linear relationship between the EC_{50} values and the serum level for several compounds. To compare with their results, we have calculated the dissolved concentration at serum level $1.81 \cdot 10^{-2}$ mol·protein m^{-3} that we would obtain with a nominal concentration of 30.6, 33.3, 39.2 and 219 μM reported in their paper as the EC_{50} values for p,p'-DDT, Dieldrin, Pentachlorophenol and 4-Chlorophenol, respectively. Then we have calculated which value of this nominal concentration would produce the same dissolved concentration as the amount of serum increases in the medium.
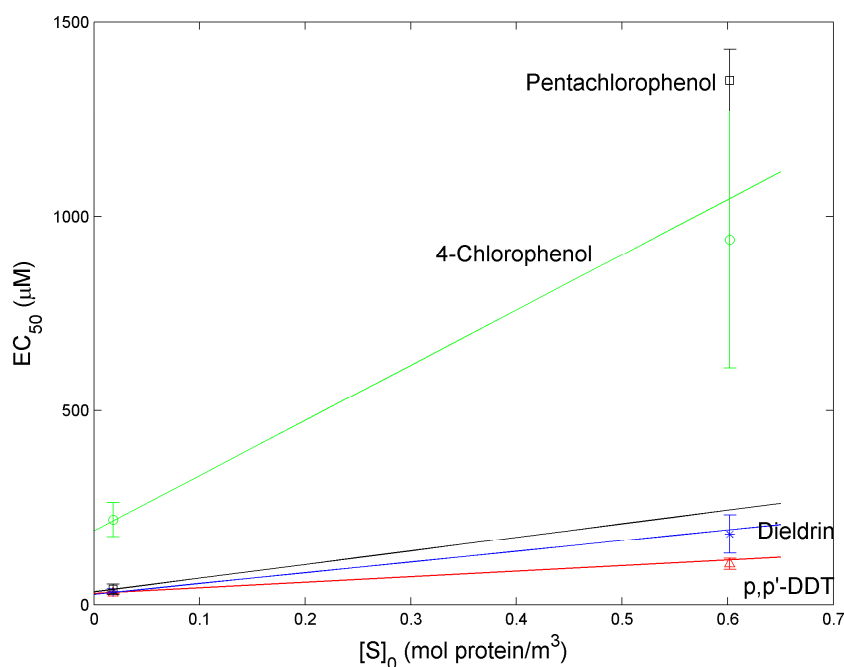
Figure 11. Relation between toxic potency of p,p'-DDT, Diledrin, 4-Chlorophenol and Pentachlorophenol -defined as the nominal concentration that produces a dissolved phase concentration equivalent to that obtained at $[S]_0 = 1.81 \cdot 10^{-2}$ mol·protein m^{-3} - and albumin concentration.

The results are summarized in Figure 11. As it can be observed the model also predicts a linear relationship between EC_{50} and serum levels as observed experimentally by Gülden et al. (2002). In

addition, the extrapolation values at high serum levels agree with the experimental values reported by Gulden et al (2002) with the exception of Pentachlorophenol, where the calculated EC$_{50}$ values are lower than the experimental ones. As pointed out by Gülden et al. (2002) this indicates the serum has no other effect than to bind the chemicals. In addition, our simulation points out that the same dissolved concentration will produce the same observed effect, in this case EC$_{50}$, therefore, serum influence can be removed from in vitro experiments by considering dissolved concentrations. The different behaviour of Pentachlorophenol, which was also clear in the results from Table 5, suggests that the binding in this case is of different nature than the non-specific binding assumed for the development of correlations for K_S.

4.3. LOOSES TROUGH THE HEADSPACE

To analyze the dynamics of looses due to volatilization and the possibility of cross contamination between wells in the plate, we have analyzed the extreme case of two wells with a common headspace, see Figure 12. We have assumed the same conditions in each well in terms of volume of liquid, number of cells and serum. Furthermore, we have placed, at the beginning of the simulation, a certain amount of a chemical compound in one well. At the end of the experiment, and assuming there are no decomposition/metabolism reactions, we will have the same concentrations in both wells. The objective is to assess how long it will take to reach the equilibrium as a function of the Henry law constant values in relation with the normal duration of a cell-based assay experiments (2-4 days).
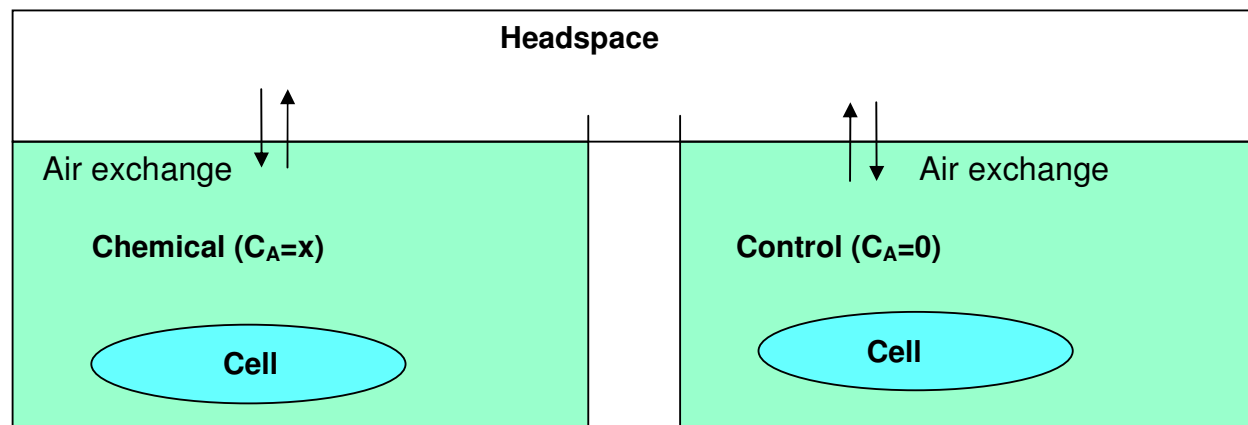

Figure 12. Simulated experiment with common headspace.

Figures 13 and 14 shows the two extreme cases for PAH as a function of the values of the Henry law constant at 37° C. As can be observed in Figure 13, for fluorene, the equilibrium is reached after only two hours of the experiment; therefore one should expect that this compound would be able to contaminate adjacent wells in experiment not performed with closed wells. Conversely, for Benzo [b] fluoranthene the time necessary to reach equilibrium is much longer that the duration of the experiment and therefore, the risk of cross contamination under normal conditions is quite low.
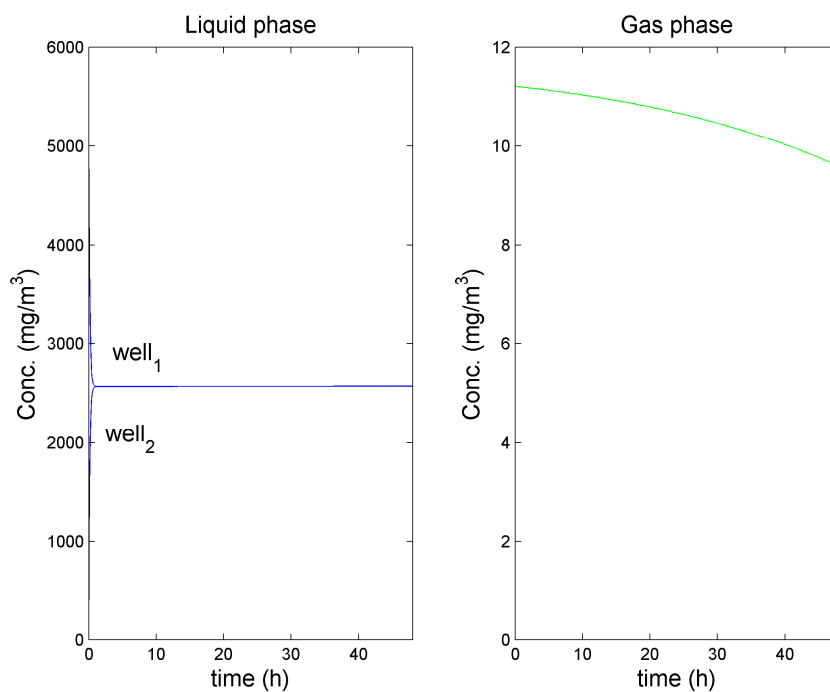
Figure 13. Simulated total concentrations for Fluorene in the liquid and gas phases of two wells with a common headspace during a 48 h experiment.
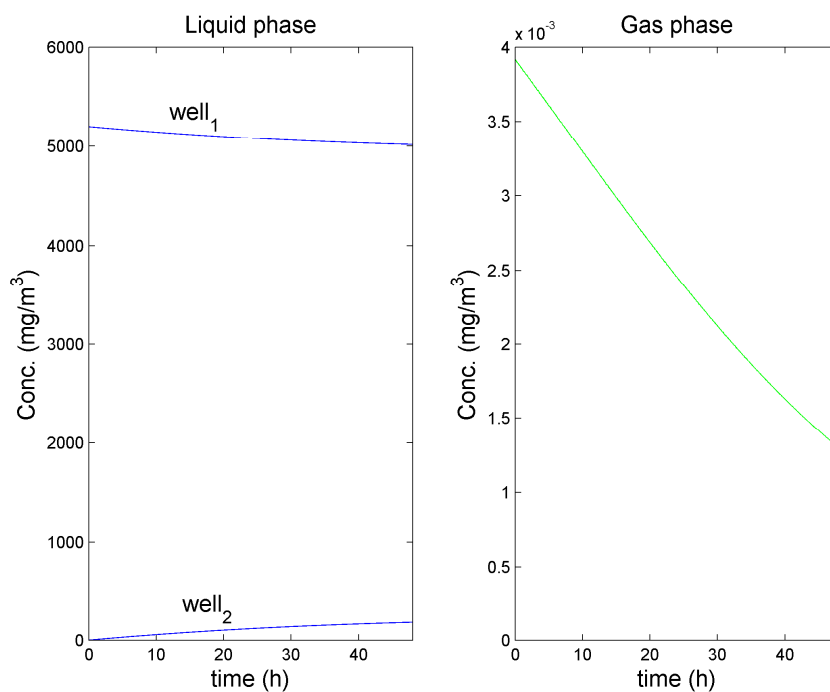
Figure 14. Simulated total concentrations for Benzo [b] fluoranthene in the liquid and gas phases of two wells with a common headspace, during a 48 h experiment.

If we assume that the experimental conditions are standard at the HTS facility and we impose a 10% limit for the losses (one should consider that the simulated case is not realistic since the wells are covered by a lid and therefore the headspace losses are less than the simulated ones) and a compound

22

with the physico-chemical properties of Phenanthrene, we can establish a limit value for the H_{37} as 0.024 Pa m^3 mol^{-1}. In a similar way, this value can be calculated for the other compounds, but the simulations show that the H value is also related to the other physico-chemical properties, mainly log K_{ow} as well as the experimental conditions.

4.4. TIME SCALES

One important assumption in this mass balance model is that sorption processes are fast compared with the other processes, i.e. the partitioning is instantaneous. To check the validity of this assumption, we have modelled the bioconcentration of compounds by 3T3 cells assuming constant uptake and depuration rates and by modelling the medium-cell exchange as shown by Del Vento and Dachs (2002).

The concentration of a compound in the 3T3 cells over time can be expressed, assuming a self-sustained cell community (no dilution effects due to growth), and a metabolism rate much lower than the depuration rate, as:

$$\frac{dC^{cell}}{dt} = k_{upt} \cdot C^{diss} - k_{dep} \cdot C^{cell} \tag{29}$$

where k_{upt} (m^3 mg^{-1} h^{-1}) and k_{dep} (h^{-1}) are the uptake and depuration rates constants. Uptake and depuration constants can be parameterized as function of bioconcentration factors of the chemical, permeability (P, m h^{-1}) of the cell membrane and specific surface area (S$_p$, m^2 kg^{-1}) (Del Vento and Dachs, 2002):

$$k_{dep} = \frac{S_p \cdot P}{BCF} \tag{30}$$
$$k_{upt} = S_p \cdot P$$

The specific surface area of 3T3 has been estimated by assuming spheric shape and a volume of 1.8±0.7 10^{-15} m^3 (Gülden et al., 2002) and a density of 1025 kg m^{-3} (Del Vento and Dachs, 2002). This gives a specific surface area (*Sp*) of 387.9 m^2 kg^{-1}.

In order to predict uptake and depuration rates it is necessary to know values for *BCF* and *P*. Since estimations of *BCF* and *P* exist only for a few number of compounds (e.g. Skoglund et al., 1996; Wallberg and Andersson, 1999; Swackhamer and Skoglund. 1993), these parameter has been calculated using empirical approximation based on the physical-chemical properties of the contaminant. For *BCF* we have used Eqs. (10)-(11). The same considerations can be made for the estimation of permeability of cell membrane and similar regressions have been proposed (Del Vento and Dachs, 2002):

log *P*= 1.340 log K_{ow} − 8.433   for log K_{ow} < 6.4   (31)

log *P*= 0.078   for log K_{ow} ≥ 6.4   (32)

Table 6 summarizes the uptake and depuration constants used in Eq. (29) to calculate the rate of change of concentrations of PAHs in 3T3 cells

Table 6. Uptake ($m^3 \cdot kg^{-1} \cdot h^{-1}$) and depuration ($h^{-1}$) constants used in the model.

Compound (PAHs)	3T3 cells	
	k_{upt}	k_{dep}
Naphthalene	0.047	0.061
Anthracene	1.74	0.121
Fluorene	0.47	0.095
Phenanthrene	1.90	0.123
Pyrene	12.50	0.176
Fluoranthene	14.59	0.182
Chrysene	87.32	0.255
Benzo [b] fluoranthene	464.22	0.351
Benzo [k] fluoranthene	464.22	0.351
Benzo [a] pyrene	177.55	0.292
Benzo [ghi] perylene	464.22	0.244
Indeno [1,2,3,cd] pyrene	464.22	0.314

Figures 15-17 show the results of the simulation of the behaviour of the internal concentration during a 48 h experiment assuming constant external concentration and zero initial internal concentration. As can be observed, even though the internal concentration reach its equilibrium value before the end of the experiment there is a transition period. Therefore, the assumption of equilibrium for the cells does not hold and a cell line dynamic model is necessary to consider this part.
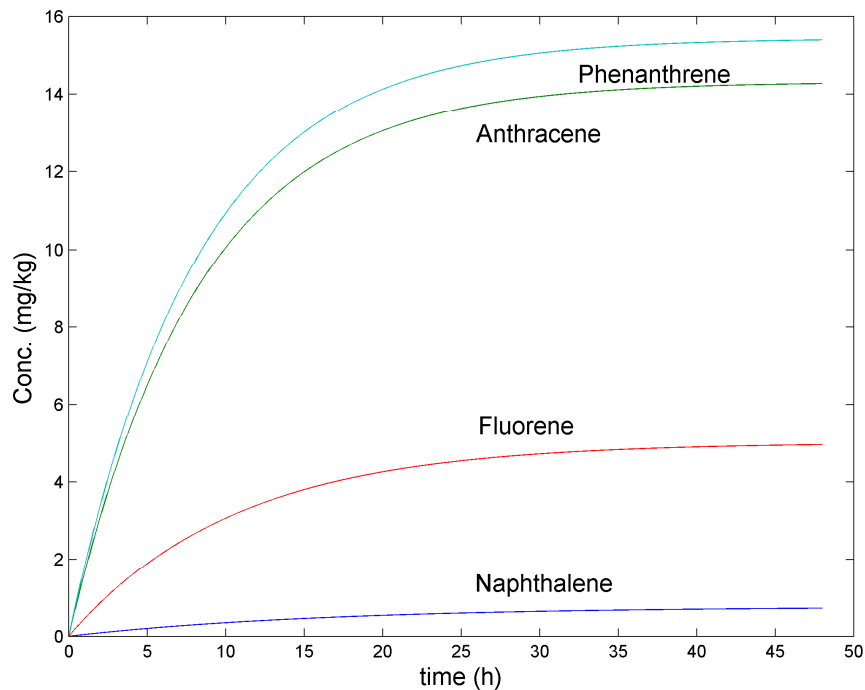

Figure 15. Simulated internal concentrations (mg kg^{-1} ww) in 3T3 for Naphthalene, Fluorene, Anthracene and Phenanthrene PAHs. $t(C = C_{final}/2)$= 10.5, 7.2, 5.7, 5.6 h , respectively.

24
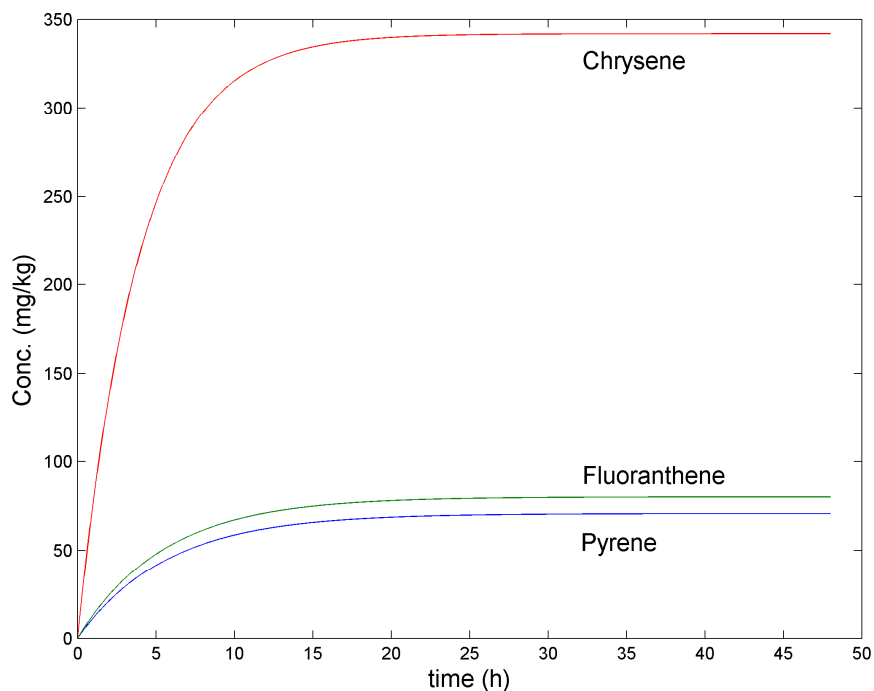
Figure 16. Simulated internal concentrations (mg kg^{-1} ww) in 3T3 for Pyrene, Fluoranthene, and Chrysene PAHs. t(C = C$_{final}$/2)= 3.9, 3.8, 2.7 h, respectively.

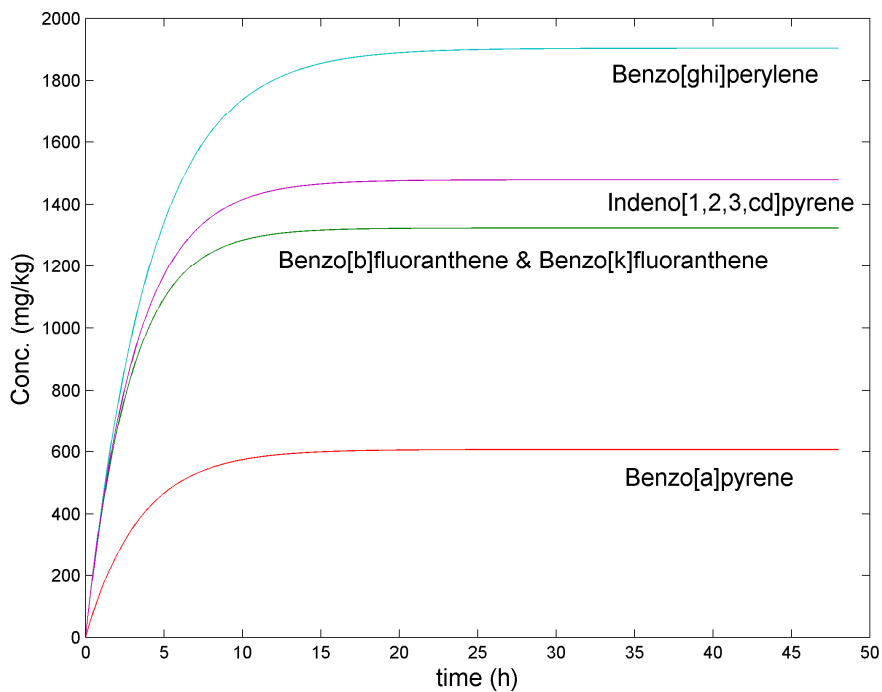Figure 17. Simulated internal concentrations (mg kg^{-1} ww) in 3T3 for Benzo[b]fluoranthene, Benzo[k]fluoranthene, Benzo[a]pyrene, Benzo[ghi]perylene and Indeno[1,2,3,cd] pyrene PAHs. t(C = C$_{final}$/2)= 1.9, 1.9, 2.4, 2.8 and 2.2 h, respectively.

Furthermore as can be observed from the internal concentrations reached; there is a correlation between log K_{ow} values and the final internal concentration. In addition, the time to reach the half value of the internal concentration is inversely proportional to the log K_{ow} until the value of 6.4 that modifies the trend and changes the form of the correlations.

5. CONCLUSIONS

A dynamical mass balance model that considers the partitioning between the medium and the headspace as well as the partitioning in the medium between plastic walls, dissolved, attached to serum and to cells, has been developed and implemented. The model predicts how much of the "nominal" concentration will contribute to the real toxicity experienced by the cells. This value depend on the physico-chemical properties of the compound, principally the octanol-water partition coefficient, K_{ow}, and the gas-liquid partition coefficient, K_{GL}. In addition, there is a typical dynamic behaviour of the dissolved concentration in the medium that decreases during the experiment due to the growth and reproduction of the cells. Consequently, even in the absence of decomposition or metabolism, the concentrations in the different compartments of the in vitro cell-based assay are changing over time.

The model is also able to predict the observed linear effect of serum concentrations on the EC_{50} value found experimentally by Gülden et al (2002) as well as to define a Henry low value above which one may expect volatilization problems. Of course, this is an arbitrary limit that should be revised using real measurements in the plates.

Finally, a model of the cell dynamics uptake and depuration rates seems necessary to consider the delays in reaching the final concentration during the 48 h experiments. Our next step would consist on the development of such a model as well as on the possibility to verify experimentally the results obtained concerning the dynamics of chemicals in the cell-based assays.

6. NOTATION

A_s medium-headspace exchange surface area, m^2,
A_l headspace losses surface area, m^2,
C Concentration, mg/m^3,
$[C]$ concentration of cell lipid in medium, kg m^{-3},
D diffusion coefficient, m^2 s^{-1},
F mass flow, mg m^{-2} s^{-1},
H Henry law constant, Pa m^3 mol^{-1},
K_C cells-medium partitioning coefficient, m^3 kg^{-1} lipid,
K_{GL} gas-liquid distribution coefficient,
K_{ow} octanol-water partition coefficient
K_P plastic-medium partitioning coefficient, m,
K_S partitioning coefficient between serum and medium, m^3 mol^{-1},
k_{AW} two film mass transfer coefficient, m s^{-1},
k_G air film mass transfer coefficient, m s^{-1},
k_L liquid film mass transfer coefficient, m s^{-1},
k reaction rate constant, s^{-1},
MW molecular weight, g/mol
P pressure, Pa,
R universal gas constant
Sc Schmidt number,
$[S]$ concentration of proteins in medium, mol m^{-3},
S_M plastic- medium exchange surface area, m^2
t time, s,
T temperature, K
V volume, m^3,

Greek symbols

ρ density, kg m^{-3},
μ viscosity, ,

Superscripts

diss   dissolved
p   plastic
S   serum
T   total

Subscripts

AW   air-water
degr   degradation
l   loses
M   medium
H   headspace

7. REFERENCES

Balaz, S. 2009. Modeling kinetics of subcellular disposition of chemicals. Chem. Rev. 109, 1793-1899.

Balls, M., Amcoff, P., Bremer, S., Casati, S., Coecke, S., Clothier, R., Combes, R., Corvi, R., Curren, R., Eskes, C., Fentem, J., Gribaldo, L., Halder, M., Hartung, T., Hoffmann, S., Schectman, L., Scott, L., Spielmann, H., Stokes, W., Tice, R., Wagner, D., Zuang, V. ECVAM. 2006. The principles of weight of evidence validation of test methods and testing strategies. The report and recommendations of ECVAM workshop 58. ATLA 34, 603–620.

Bamford, H.A., Poster, D.L., Baker, J.E. 1999. Temperature dependence of Henry's law constants of thirteen polycyclic aromatic hydrocarbons between 4° C and 31° C. Environmental Toxicology and Chemistry 18, 1905-1912.

Blaise, C., Legault, R., Bermingham, N., Van Coillie, R., Vasseur, P. 1986. A simple microplate algal assay technique for aquatic toxicity assessment. Toxic. Assess. 1, 261-281.

Bouhifd, M. and Whelan, M. 2006. Automated 3T3/NRU standard operating protocol for acute cytotoxicity testing of chemicals. European Commission, JRC, IHCP, InVitech Deliverable No. D2.1.

Bouhifd, M., Casado, J., Coecke, S. *et al.* 2005. Automated process for 3T3/NRU cytotoxicity assay. European Commission, JRC, IHCP.

Bouhifd M, Norlen H, Bories G, Whelan M, Casado Poblador J, Parissis N, Coecke S. Automation and Performance Assessment of a Basal Cytotoxicity Assay Intended for Regulatory Safety Assessment. ADMET Europe 2008 Conference; 19 February 2008; Stockholm (Sweden).

Carafa, R., Marinov, D., Dueri, S., Wollgast, J., Ligthart, J., Canuti, E., Viaroli, P. and Zaldívar, J. M., 2006. A 3D hydrodynamic fate and transport model for herbicides in Sacca di Goro coastal lagoon (Northern Adriatic). Mar. Poll. Bull. 52, 1231-1248.

DeBruyn, A.M.H. and Gobas, F.A.P.C. 2007. The sorptive capacity of animal protein. Environmental Toxicology and Chemistry 26, 1803-1808.

DeJongh, J., Forsby, A., Houston, J.B., Beckman, M., Combes, R., Blaauboer, B.J., 1999. An integrated approach to the prediction of systemic toxicity using computer-based biokinetic models and biological *in vitro* test methods: Overview of a prevalidation study based on the ECITTS Project. Toxicology in Vitro 13, 549-554.

Del Vento, S. and Dachs, J., 2002. Prediction of uptake dynamics of persistent organic pollutants by bacteria and phytoplankton. Environmental Toxicology and Chemistry 21, 2099-2107.

Dueri, S. Castro-Jimenez, J. and Zaldívar J.M., 2008. On the use of the partitioning approach to derive Environmental Quality Standards (EQS) for persistent organic pollutants (POPs) in sediments: A review of existing data. Science of the Total Environment 403, 23-33.

Dueri, S., Dallhof, I., Hjorth, M., Marinov, D., and Zaldívar, J.M., 2009. Modelling the combined effects of nutrients and pyrene on the plankton population: Validation using mesocosm experimental data and scenario analysis. Ecol. Model. 220, 2060-2067.

Eisentraeger,A., Dott, W., Klein, J., Hahn, S. 2003. Comparative studies on algal toxicity testing using fluorometric microplate and Erlenmeyer flask growth-inhibition assays. Ecotoxicol. Environ. Saf. 54, 346-354.

Fuller, E.N., Schettler, P.D. and Giddings, J.C. 1966. A new method for prediction of binary gas phase. diffusion coefficients. Ind. Eng. Chem. 58, 18-27.

Gross, M., Daginnus, K., Deviller, G., de Wolf, W., Dungey, S., Galli, C., Gourmelon, A., Jacobs, M., Matthiessen, P., Micheletti, C., Nestmann, E., Pavan, M., Paya-Perez, A., Ratte, H.-T., Safford, B., Sokull-Kluttgen, B., Stock, F., Stolzenberg, H.-C., Wheeler, J, Willuhn, M., Worth, A., Zaldívar, J.M. and Crane, M. 2010. Thresholds of Toxicological Concern for Endocrine Active Substances in the Aquatic Environment. *Integrated Environmental Assessment and Management* **6**, 2-11.

Gubbels-van Hal, W.M.L.G., Blaauboer, B.J., Barentsen, H.M., Hoitink, M.A., Meerts, I.A.T.M. and van der Hoeven, J.C.M. 2005. An alternative approach for the safety evaluation of new and existing chemicals, an exercise in integrated testing. Regulatory Toxicology and Pharmacology 42, 284-295.

Gülden, M., Mörchel, S. and Seibert, H. 2001. Factors influencing nominal effective concentrations of chemical compounds *in vitro*: cell concentration. Toxicology *in vitro* 15, 233-243.

Gülden M. and Seibert, H. 2003. *In vitro-in vivo* extrapolation: Estimation of human serum concentrations of chemicals equivalent cytotoxic concentrations *in vitro*. Toxicology 189, 211-222.

Heijne, W.H.M., Kienhuis, A. S., van Ommen, B., Stierum, R.H. and Groten, J.P. 2005. Systems toxicology: applications of toxicogenomics, transcriptomics, proteomics and metabolomics in toxicology. Expert Rev. Proteomics 2, 767-780.

Heringa, M. B., Schreurs, R.H.M.M., Busser, F., van der Saag, P.T., van der Burg, B., Hermens, J.L.M. 2004. Towards more useful in vitro toxicity data with measured free concentrations. Environ. Sci. Technol. 38, 6263-6270.

Hestermann, E.V., Stegeman, J.J., Hahn, M.E. 2000. Serum alters the uptake and relative potencies of halogenated aromatic hydrocarbons in culture cell assays. Toxicol. Sci. 53, 316-325.

Höfer, T., Gerner, I., Gundert-Remy U., Liebsch, M., Schulte, A., Spielmann, H., Vogel, R., Wettig, K. 2004. Animal testing and alternative approaches for he human health risk assessment under the proposed new European chemicals legislation. Arch. Toxicol. 78, 549-564.

International Agency for Research on Cancer (IARC), 1991. Monographs on the evaluation of carcinogenic risks to humans. Vols. 43-53. Lyon.

ICCVAM, 2006a. In Vitro Cytotoxicity Test Methods for Estimating Acute Oral Systemic Toxicity. Background Review Document. Volumes 1 and 2 (of 2). Interagency Coordinating Committee on the Validation of Alternative Methods (ICCVAM), National Toxicology Program (NTP), Interagency Center for the Evaluation of Alternative Toxicological Methods (NICEATM), National Institute of Environmental Health Sciences (NIEHS), National Institutes of Health, U.S. Public Health Service, Department of Health and Human Services, November 2006, NIH Publication No. 07-4518.

ICCVAM, 2006b. Test Method Evaluation Report (TMER). In Vitro Cytotoxicity Test Methods for Estimating Starting Doses for Acute Oral Systemic Toxicity. Interagency Coordinating Committee on the Validation of Alternative Methods (ICCVAM), National Toxicology Program (NTP), Interagency Center for the Evaluation of Alternative Toxicological Methods (NICEATM), National Institute of Environmental Health Sciences (NIEHS), National Institutes of Health, U.S. Public Health Service, Department of Health and Human Services, November 2006, NIH Publication No. 07-4519.

Jonker, M.T.O., van der Heijden, S.A. 2007. Bioconcentration factor hydrophobicity cutoff: An artificial phenomenon reconstructed. Environ. Sci. Technol. 41, 7363-7369.

Jurado, E., Zaldivar, J.M., Marinov, D. and Dachs, J. 2007. Fate of persistent organic pollutants in the water column: Does turbulent mixing matter? Mar. Poll. Bull. 54, 441-451.

Kanwisher, J. 1963. Effect of wind on CO_2 exchange across the sea surface. J. Geophys. Res 68, 3921-3927.

Kramer, N. I. 2010. Measuring, modelling and increasing the free concentration of test chemicals in cell assays. PhD Thesis. Utrecht University.

Lilienblum, W., Dekant, W., Foth, H., Gebel, T., Hengstler, J.G., Kahl, R., Kramer, P.-J., Schweinfurth,H., Wollin, K.-M. 2008. Alternative methods to safety studies in experimental animals: role in the risk assessment of chemicals under the new European Chemicals Legislation (REACH). Arch. Toxicol. 82, 211-236.

Mackay, D. and Hickie, B. 2000. Mass balance model of source apportionment, transport and fate of PAHs in Lac Saint Louis, Quebec. Chemosphere 41, 681-692.

Marinov, D. Dueri, S., Puillat, I., Carafa, R., Jurado, E., Berrojalbiz, N. Dachs, J. and Zaldívar, J.M., 2009. Integrated modeling of Polycyclic Aromatic Hydrocarbons (PAHs) in the marine ecosystem: Coupling of hydrodynamic, fate and transport, bioaccumulation and planktonic food web models. Marine Pollution Bulletin 58, 1554-1561.

National Research Council (NRC) of the National Academies. 2007. Toxicity Testing in the 21st Century: A vision and a strategy. Committee on Toxicity Testing and Assessment of Environmental Agents. The National Academies Press, Washinton DC, USA.

Norlén, H., Bouhifd, M., Bories, G., Whelan, M., Casado, J., Parissis, N. Fernando F., Coecke, S. 2007. Report on 3T3/NRU assay results for the testing period January-April 2007. JRC 43733. pp 27.

OECD. 1993. Guidance document for the development of OECD guidelines for the testing of chemicals. OECD Monograph N[o] 76, Paris.

Paasivirta, J., Sinkkonen, S., Mikkelson, P., Rantio, T. and Wania, F., 1999. Estimation of vapor pressures, solubilities and Henry's laws constants of selected persistent organic pollutants as functions of temperature. Chemosphere 39: 811-832.

Perry and Chilton 1984.Chemical Engineering Handbook, 6th Ed. McGraw-Hill. New York.

Riedl, J., Altenburger, R. 2007. Physicochemical substance properties as indicators for unreliable exposure in microplate-based bioassays. Chemosphere 67, 2210-2220.

Schwarzenbach, R. P., Gschwend, P. M., Imboden, D. M., 2003, Environmental Organic Chemistry, 2nd Edition, Wiley Interscience, New York.

Simpson, S. L., Roland, M.G.E., Stauber, J.L., Batley, G.E., 2003. Effects of declining toxicant concentrations on algal bioassay endpoints. Environ. Toxicol. Chem. 22, 2073-2079.

Skoglund, R.S. K. Stange, and D.L. Swackhamer. 1996. A kinetics model for predicting the accumulation of PCBs in phytoplankton. Environ. Sci. Technol. 30, 2113–2120.

Stange, K. and Swackhamer, D. L. 1994. Factors affecting phytoplankton species-specific differences in accumulation of 40 polychlorinated biphenyls (PCBs). Environ. Toxicol. Chem. 11, 1849-1860.

Swackhamer, D.L. and R.S. Skoglund. 1993. Bioaccumulation of PCBs by phytoplankton: kinetics vs. equilibrium. Environ Toxicol Chem 12, 831-838.

Thellen, C., Balise,C., Roy, Y.H.C. 1989. Round robin testing with the *Selenastrum capricornutum* microplate toxicity assay. Hydrobiologia 188/189, 259-268.

U.S. EPA, 2003. A framework for a computational toxicology research program. Washington D.C. EPA600/R-03/65.

van Leeuwen, C.J., Patlewicz, G.Y., Worth, A.P., 2007. Intelligent testing strategies. In: van Leeuwen, C.J., Vermeire, T.G. (Eds.), Risk Assessment of Chemicals: An Introduction, second ed. Springer, AA Dordrecht, The Netherlands (P.O. Box 17, 3300), ISBN 978-1-4020-6101-1(HB).

Wallberg, P. and Andersson, A. 1999. Determination of adsorbed and absorbed polychlorinated biphenyls (PCBs) in seawater microorganisms. Marine Chemistry 64, 287-299.

Waters, M., Boorman, G. Bushel, P., Cunningham, M., Irwin, R., Merrick, A., Olden, K., Paules, R., Selkirk, J., Stasiewicz, S., Weis, B. Van Houten,B., Walker, N. and Tennant, R. 2003. Systems

toxicology and the chemical effects in biological systems (CEBS) knowledge base. Environmental Health Perspectives 111, 811-824.

Westerterp, K. R., van Swaaij, W.P.M. and Beenackers A.A.C.M. 1984. Chemical reactor design and operation. John Wiley & sons. Chichester pp 800.

Wilke, C.R., Chang, P., 1955. Correlation of diffusion coefficients in dilute solutions. Am Inst. Chem. Eng. J. 1: 264–270.

Worth, A.P., 2004. The tiered approach to toxicity assessment based on the integrated use of alternative (non-animal) tests. In: Cronin, M.T.D., Livingstone, D.J. (Eds.), Predicting Chemical Toxicity and Fate. CRC Press, Boca Raton, FL, USA, pp. 389–410.

Abstract. There is a need to integrate existing *in vitro* dose-response data in a coherent framework for extending their domain of applicability as well as their extrapolation potential. This integration would contribute towards the reduction of animal use in toxicology by using *in vitro* data for quantitative risk assessment; moreover it would reduce costs and time especially when such approaches would be used for dealing with complex human health and ecotoxicological endpoints. In this work, based on HTS (High Throughput Screening) *in vitro* data, we have assessed the advantages that a dynamic biology-toxicant fate coupled model for *in vitro* cell-based assays could provide when assessing toxicity data, in particular, the possibility to obtain the dissolved (free) concentration which can help in raking the toxicity potency of a chemical and improve data reconciliation from several sources taking into account the inherent variability of cell-based assays. The results show that this approach may open a new way of analyzing this type of data sets and of extrapolating the values obtained to calculate *in vivo* human toxicology thresholds.

How to obtain EU publications

Our priced publications are available from EU Bookshop (http://bookshop.europa.eu), where you can place an order with the sales agent of your choice.

The Publications Office has a worldwide network of sales agents. You can obtain their contact details by sending a fax to (352) 29 29-42758.

The mission of the JRC is to provide customer-driven scientific and technical support for the conception, development, implementation and monitoring of EU policies. As a service of the European Commission, the JRC functions as a reference centre of science and technology for the Union. Close to the policy-making process, it serves the common interest of the Member States, while being independent of special interests, whether private or national.

JRC
EUROPEAN COMMISSION

Publications Office
Publications.eu.int

9 789279 158001

35